

## ARTICLES

## Evidence of Extended Solidlike Layering in [Bmim][NTf2] Ionic Liquid Thin Films at Room-Temperature

Simone Bovio,<sup>†</sup> Alessandro Podestà,<sup>\*,†</sup> Cristina Lenardi,<sup>‡</sup> and Paolo Milani<sup>†</sup>

*C.I.Ma.I.Na. and Dipartimento di Fisica, Università degli Studi di Milano, via Celoria 16, 20133, Milano, Italy, and C.I.Ma.I.Na. and Istituto di Fisiologia Generale e Chimica Biologica, Università degli Studi di Milano, via Trentacoste 2, 20134, Milano, Italy*

*Received: January 26, 2009*

We report the direct observation of solidlike ordering at room temperature of thin films of [Bmim][NTf2] ionic liquid on mica, amorphous silica, and oxidized Si(110). A statistical quantitative analysis of atomic force microscopy topographies shows that on these surfaces [Bmim][NTf2] forms layered structures, characterized by a perpendicular structural periodicity of  $\sim 0.6$  nm. Remarkably, even the highest structures, up to 50 nm high, behave solidlike against the AFM probe. Conversely, on highly oriented pyrolytic graphite the ionic liquid forms nanometer-sized, liquidlike domains. The results of this study are directly relevant for those applications where ILs are employed in form of thin films supported on solid surfaces, such as in microelectromechanical or microelectronic devices. More generally, they suggest that at the liquid/solid interface the structural properties of ILs can be far more complex than those depicted so far, and prompt new fundamental investigations of the forces that drive supported ILs through a liquidlike-to-solidlike transition.

## Introduction

Room-temperature ionic liquids (ILs)<sup>1,2</sup> are receiving a rapidly increasing interest as alternatives to conventional electrolytes that can boost the performances of photoelectrochemical devices used for energy storage and energy production such as supercapacitors<sup>3</sup> or Graetzel solar cells.<sup>4</sup> Moreover, ILs are considered as a promising new class of lubricants in miniaturized as well as in macroscopic mechanical systems.<sup>5,6</sup> In all these cases, the most relevant processes determining the performance of the devices take place at the liquid/solid interface between ILs and solid surfaces: this is a region only a few nanometers thick where the properties of ILs can be significantly different from those of the bulk. The investigation of the interfacial properties of ILs is therefore of primary importance for their technological exploitation.

To date, the (bulk)liquid–vapor and solid–(bulk)liquid ILs interfaces have been studied, mostly by sum-frequency generation spectroscopy,<sup>7–11</sup> by X-ray photoemission spectroscopy,<sup>12,13</sup> and by a combination of these and other surface science techniques,<sup>14–18</sup> including atomic force microscopy (AFM).<sup>19,20</sup> For imidazolium-based ILs, ordering of the cations at the solid/liquid or liquid/vapor interface has been inferred from vibrational spectroscopy data. Sloutskin et al.<sup>15</sup> inferred from X-ray reflectivity data of imidazolium-based ILs the existence of an ordered surface layer at the liquid/vapor interface, about 0.6–0.7 nm thick, composed by both cations and anions. Very recently, Mezger et al. performed a similar study of the (bulk)liquid/solid interface between a negatively charged sapphire substrate

and imidazolium and pyrrolidinium-based ILs.<sup>21</sup> They found strong interfacial layering, with repeated spacing of 0.7–0.8 nm, decaying exponentially into the bulk liquid. Moreover, the existence of periodically ordered layers of ILs, including an imidazolium-based, at the (bulk)liquid/solid interface with mica and silica, has been recently reported by Atkin et al.,<sup>20</sup> and interpreted as solvation layers. Despite these interesting results, the knowledge of the structural properties of ILs at interfaces, in particular with solid surfaces, is still very poor and important questions are still waiting to be answered. Researchers still do not know whether, and how far, the ordered layers extend into the bulk of the liquid, nor do they know how the cation–anion pairs are organized within each layer, and what is the phase (liquid, solidlike) of the IL in the ordered region. A better understanding of the behavior of ILs at interfaces can be achieved studying systems where the surface to volume ratio is very large, as in very thin supported films. To date, this is a largely unexplored field, since all the above-mentioned studies were conducted on systems where a bulk amount of IL was present right above, or below, the interface.

In this communication, we report on the direct observation by tapping-mode AFM of nanoscale morphological and structural properties of very thin coatings of 1-butyl-3-methylimidazolium bis(trifluoromethylsulfonyl)imide, [Bmim][NTf2], on different surfaces of technological interest. Our work significantly expands the preliminary work of Liu et al., who recently reported about the layering at room-temperature of an imidazolium-based IL, [Bmim][PF6], on mica.<sup>22</sup> Using AFM, we have visualized nanoscale structures of [Bmim][NTf2] on a variety of surfaces: mica, amorphous silica, polished, oxidized p-doped Si(110), and highly oriented pyrolytic graphite (HOPG). Applying a rigorous protocol for the statistical analysis of AFM images we have characterized the structural properties of IL

\* To whom correspondence should be addressed. E-mail: alessandro.podesta@mi.infn.it.

<sup>†</sup> C.I.Ma.I.Na. and Dipartimento di Fisica.

<sup>‡</sup> C.I.Ma.I.Na. and Istituto di Fisiologia Generale e Chimica Biologica.

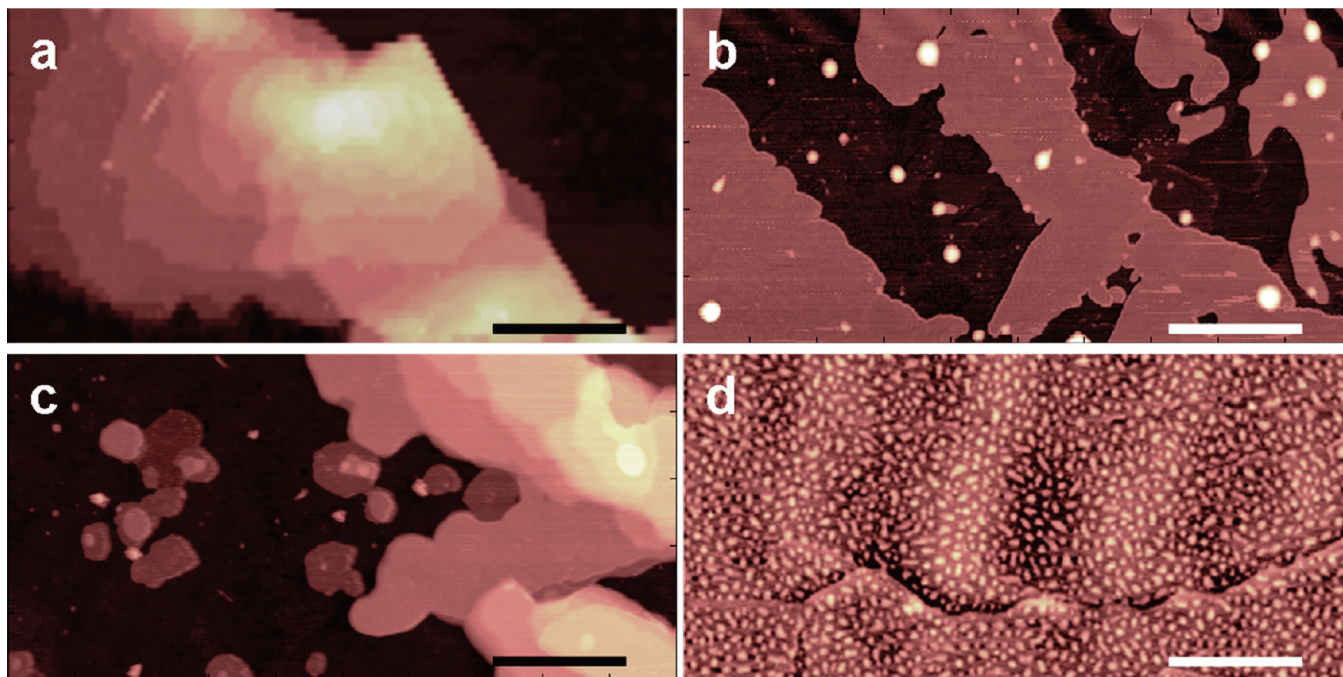


**Figure 1.** AFM topographies of thin [Bmim][NTf<sub>2</sub>] coatings on different substrates: (a) polished oxidized Si(110); (b) mica; (c) amorphous silica; (d) HOPG. Vertical scales: (a,b) 50; (c) 90; (d) 10 nm. Scale bars: 1  $\mu$ m.

films, validating a structural model where [Bmim][NTf<sub>2</sub>] forms layered solidlike structures at room-temperature on mica and silica surfaces, with a basic periodicity in the perpendicular direction of  $\sim 0.6$  nm. In contrast, on HOPG [Bmim][NTf<sub>2</sub>] segregates in nanometer-sized domains.

### Experimental Methods

[Bmim][NTf<sub>2</sub>] thin films are prepared by spotting a 20  $\mu$ L droplet of [Bmim][NTf<sub>2</sub>]-methanol solution on mica, highly oriented pyrolytic graphite (HOPG), amorphous silica, and polished, oxidized p-doped Si(110) substrates, and allowing methanol to completely evaporate in air, leaving behind IL layers and/or droplets. Methanol with 99.8% (HPLC) purity grade was used. The IL concentration in the deposition solution was typically kept below  $1 \times 10^{-3}$  mg/mL. To make the methanol evaporation process slower and obtain more uniform coatings and thicker structures, the specimens were cured in a saturated methanol atmosphere during evaporation. A comparative X-ray photoelectron spectroscopy analysis of pure and methanol-mixed [Bmim][NTf<sub>2</sub>] confirmed that the solvent used in the deposition process does not react with [Bmim][NTf<sub>2</sub>] (see Supporting Information, Figures S1 and S2).

Substrates were freshly prepared immediately before deposition of the [Bmim][NTf<sub>2</sub>]-methanol solution. Mica and HOPG were stripped with adhesive tape in order to obtain atomically smooth, clean surfaces. Discs (13 mm-diameter) of amorphous silica (glass coverslips) and squared specimens of polished, oxidized Si(110) were cured in aqua-regia solution (HCl–HNO<sub>3</sub> from, respectively, 37% and 69.5% solutions at ratio 3:1) before use, to remove organic contaminants and rehydroxylize the surface.

A Bioscope II–Nanoscope V AFM from Veeco Instruments was used. The AFM was operated in tapping mode in air with standard single-crystal silicon cantilevers (resonance frequency between 200 and 300 kHz, nominal radius of curvature of the tip, 5–10 nm). Typically, image scan size was between 5  $\mu$ m  $\times$  5  $\mu$ m and 20  $\mu$ m  $\times$  20  $\mu$ m, with scan rates in the range

0.5–1.5 Hz. Stable imaging conditions could be achieved and maintained for hours as if scanning on a solid surface. We did not observe significant changes in the imaging conditions when imaging in a dry nitrogen atmosphere. AFM raw data have been analyzed according to the statistical protocol described in the Supporting Information.

### Results and Discussion

Figure 1 shows a collection of representative AFM topographies of thin coatings of [Bmim][NTf<sub>2</sub>] on polished oxidized Si(110), mica, amorphous silica, and HOPG. Figure 1a–c show layered structures, characterized by lateral dimensions in the 1–20  $\mu$ m range, and height above 50 nm in some cases. While the average height of terraces is similar on the three substrates, on silica substrates [Bmim][NTf<sub>2</sub>] shows a more pronounced tendency to grow three-dimensionally than on mica. No evidence of ordered extended structures could be found on HOPG substrates (Figure 1d). On HOPG only nanometer-sized, rounded domains (nanodroplets) of IL spontaneously form upon evaporation of methanol. Coexistence of submicrometer droplets and layers is observed occasionally on amorphous silica and mica, and very rarely on oxidized Si(110) surfaces. No changes in the shape of layered features were typically observed after repeated scanning of the same areas, if not occasionally, when working with high forces. When imaged by AFM, such structures, even the highest, behave like solid surfaces. AFM phase-imaging (Figure S3 in the Supporting Information) also suggests that the phase of IL in layered structures and droplets is different. The observed layers have been imaged also after several months, and no changes in their average structure and morphology have been observed, demonstrating that such structures are extremely stable even in ambient (humid) conditions.

A statistical analysis of the AFM images provided quantitative information on the structural properties of [Bmim][NTf<sub>2</sub>] films (see Supporting Information for the details). We investigated whether the layers observed in Figure 1a–c could result from

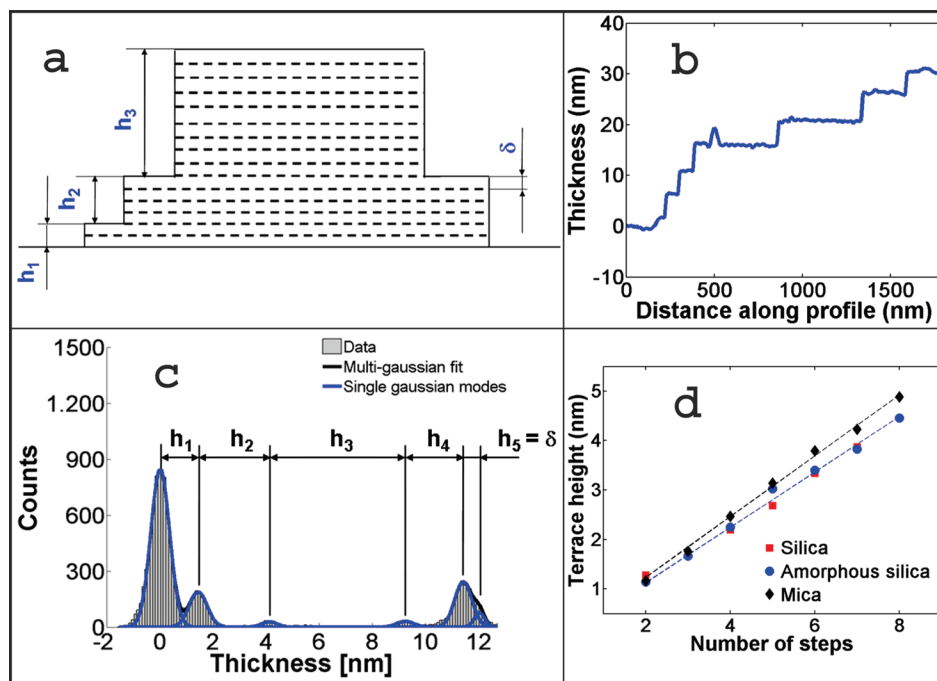


**Figure 2.** (a) Structural model of layered structures, consisting in the stacking of a molecular layer with thickness  $\delta$  resulting in terraces with different heights  $h_1, h_2, \dots$  (b) Representative AFM topographic profile of a layered structure. (c) Typical height histogram of a layered structure. Peak-to-peak distances represent terrace heights. (d) Correlation between average terrace heights measured on different surfaces and the number of basic steps in each terrace, obtained by fitting structural data (error bars are comparable to marker size).

the regular vertical arrangement of a molecular layer with thickness  $\delta$ . According to the structural model shown in Figure 2a, we made the hypothesis that each terrace consists of several basic layers, and terraces with different heights are stacked one on top of the other. This model well represents the typical AFM profiles of layered structures (one is shown in Figure 2b). To characterize statistically and accurately the heights of the observed terraces, we considered the histograms of the heights in AFM topographies of layered structures. Figure 2c shows a typical height histogram of a layered structure. Such histograms consist of a series of peaks, each corresponding to a plateau in the AFM image. The peak-to-peak distances represent the average heights of piled-up terraces. We performed an optimization procedure on terrace heights data in order to find the best value of  $\delta$  for the different substrates. We found  $\delta = 0.61 \pm 0.01$ ,  $0.56 \pm 0.02$ , and  $0.56 \pm 0.02$  nm for mica, polished oxidized Si(110), and amorphous silica, accordingly. Figure 2d shows the curves obtained plotting the average heights of the terraces versus the ratio of these heights to  $\delta$ , approximated to the closest integer; this ratio representing the number of basic steps in each terrace. The good linear correlation of data reflects the good vertical structural order of [Bmim][NTf2] films on mica and silica substrates. Remarkably, these results are in good agreement with the results of numerical simulations of thin [Bmim][NTf2] and [Bmim][PF6] films on silica.<sup>23</sup>

Nanometer-sized heterogeneities have been observed in the bulk liquid phase of imidazolium-based ILs,<sup>24,25</sup> and interpreted as the result of the segregation of the nonpolar alkyl chains, separated by thin layers of cations paired to anions (a sort of micellization). The size of these locally ordered domains turned out to be roughly twice the length of the alkyl tail plus the cation–anion pair, scaling linearly with the number of CH<sub>2</sub> units in the alkyl chain. This scheme however is not appropriate to explain what we have observed on silica and mica surfaces, where the presence of the surface likely plays a fundamental role. The (bulk)liquid/solid interface of imidazolium and pyr-

rolidinium-based ILs on a negatively charged sapphire surface recently studied by Mezger et al. represents a system that is closer to our case.<sup>21</sup> The authors explained the observed extended interfacial layering of ILs as due to the combined effect of a net surface charge and the absence of screening of charged ions, which drive the self-assembling of charged double layers. On noncharged, nonpolar surfaces, like graphite, the alkyl tails of the cations very likely interact with the surface, hampering the stable ordering of correlated positively and negatively charged layers, therefore favoring the liquid phase. Similar arguments are invoked by Atkin et al. for explaining the observation by AFM of solvation force profiles of ILs, including an imidazolium-based, at the (bulk)liquid/solid interface with mica, silica, and graphite.<sup>20</sup> Similarly to the charged sapphire surface, the silica and mica surfaces used in our study have a negative charge. It is worth noting however that none of the works cited above provide information about the lateral extension of the ordered domains at the solid/liquid interface, while we have observed on silica and mica surfaces that the lateral dimensions of the layered domains are finite, typically in the 1–20  $\mu\text{m}$  range. Moreover, we have shown that solidlike, ordered terraces typically a few nanometers thick grow on top of each other, forming ziggurat-like structures, more than 50 nm tall, despite the fact that with the same amount of IL deposited it would be possible to cover uniformly the substrate with a single terrace. This experimental evidence requires a more complex interpretation scheme than the one presented above and stimulate new investigations of the solid/liquid interface of supported ILs.

## Conclusions

We have shown that when a few monolayers of [Bmim][NTf2] are deposited on a variety of surfaces, the whole ionic liquid rearranges in a solidlike phase, characterized by the stacking of a basic layer with thickness compatible to the size of the



cation–anion pair. Structural order is maintained up to distances corresponding to much more than the single or the few molecular layers recently observed at the interface between a bulk amount of IL and a solid surface,<sup>20,21</sup> or air.<sup>15</sup> With respect to what was reported by Liu et al. for [Bmim][PF6] on mica,<sup>22</sup> where only the molecularly thin layers appeared to be solidlike, we have observed in the case of [Bmim][NTf2] that even the highest structures behave solidlike against the AFM probe on all the substrates.

Our findings highlight the potentialities of atomic force microscopy for the quantitative investigation of the interfacial properties of thin ILs coatings. The results of this study are directly relevant for those applications where ILs are employed in the form of thin films supported on solid surfaces, such as in microelectromechanical or microelectronic devices. More generally, they suggest that at the (bulk)liquid/solid interface the structural properties of ILs can be far more complex than those depicted so far and prompt new fundamental investigations of the forces that drive supported ILs through a liquidlike-to-solidlike transition.

**Acknowledgment.** We thank P. Ballone and M. Del Pópolo for discussions and suggestions, K. Seddon and M. Deetlefs for having provided the ILs used in this study, and M. Perego for the XPS analysis of our samples. This work has been supported by Fondazione Cariplo under grant “Materiali e tecnologie abilitanti 2007”.

**Supporting Information Available:** X-ray photoelectron spectroscopy of [Bmim][NTf2]; statistical analysis of AFM data; AFM phase imaging of layers and droplets. This material is available free of charge via the Internet at <http://pubs.acs.org>.

## References and Notes

- (1) Welton, T. *Chem. Rev.* **1999**, 99, 2071–2083.
- (2) Holbrey, J. D.; Seddon, K. R. *Clean Products and Processes* **1999**, 1, 223–236.

- (3) Frackowiak, E.; Lota, G.; Pernak, J. *Appl. Phys. Lett.* **2005**, 86, 164104–1/3.
- (4) Kuang, D.; Wang, P.; Ito, S.; Zakeeruddin, S. M.; Grätzel, M. *J. Am. Chem. Soc.* **2006**, 128, 7732–7733.
- (5) Qu, J.; Truhan, J. J.; Dai, S.; Luo, H.; Blau, P. J. *Tribol. Lett.* **2006**, 22, 207–214.
- (6) Nainapampil, J. J.; Eapen, K. C.; Sanders, J. H.; Voevodin, A. A. *J. Microelectromech. Syst.* **2007**, 16, 836–843.
- (7) Fitchett, B. D.; Conboy, J. C. *J. Phys. Chem. B* **2004**, 108, 20255–20262.
- (8) Romero, C.; Baldelli, S. *J. Phys. Chem. B* **2006**, 110, 6213–6223.
- (9) Santos, C. S.; Baldelli, S. *J. Phys. Chem. B* **2007**, 111, 4715–4723.
- (10) Romero, C.; Moore, H. J.; Lee, T. R.; Baldelli, S. *J. Phys. Chem. C* **2007**, 111, 240–247.
- (11) Rollins, J. B.; Fitchett, B. D.; Conboy, J. C. *J. Phys. Chem. B* **2007**, 111, 4990–4999.
- (12) Caporali, S.; Bardi, U.; Lavacchi, A. *J. Electron Spectrosc. Relat. Phenom.* **2006**, 151, 4–8.
- (13) Gottfried, J. M.; Maier, F.; Rossa, J.; Gerhard, D.; Schulz, P. S.; Wasserscheid, P.; Steinrück, H.-P. *Z. Phys. Chem.* **2006**, 220, 1439–1453.
- (14) Imori, T.; Iwahashi, T.; Kanai, K.; Seki, K.; Sung, J.; Kim, D.; Hamaguchi, H.-o.; Ouchi, Y. *J. Phys. Chem. B* **2007**, 111, 4860–4866.
- (15) Sloutskin, E.; Ocko, B. M.; Tamam, L.; Kuzmenko, I.; Gog, T.; Deutsch, M. *J. Am. Chem. Soc.* **2005**, 127, 7796–7804.
- (16) Hoff, O.; Bahr, S.; Himmerlich, M.; Krischok, S.; Schaefer, J. A.; Kemper, V. *Langmuir* **2006**, 22, 7120–7123.
- (17) Krischok, S.; Eremtchenko, M.; Himmerlich, M.; Lorenz, P.; Uhlig, P.; Neumann, A. *J. Phys. Chem. B* **2007**, 111, 4801–4806.
- (18) Smith, E. F.; Rutten, F. J. M.; Villar-Garcia, I. J.; Briggs, D.; Licence, P. *Langmuir* **2006**, 22, 9386–9392.
- (19) Nainapampil, J. J.; Phillips, B. S.; Eapen, K. C.; Zabinski, J. S. *Nanotechnology* **2005**, 16, 2474–2481.
- (20) Atkin, R.; Warr, G. G. *J. Phys. Chem. C* **2007**, 111, 5162–5168.
- (21) Mezger, M.; Schröder, H.; Reichert, H.; Schramm, S.; Okasinski, J. S.; Schöder, S.; Honkimäki, V.; Deutsch, M.; Ocko, B. M.; Ralston, J.; Rohwerder, M. *Science* **2008**, 322, 424–428.
- (22) Liu, Y.; Zhang, Y.; Wu, G.; Hu, J. *J. Am. Chem. Soc.* **2006**, 128, 7456–7457.
- (23) Del M., Pópolo, Ballone, P. Private communication, 2009.
- (24) Triolo, A.; Russina, O.; Bleif, H.-J.; Di Cola, E. *J. Phys. Chem. B* **2007**, 111, 4641–4644.
- (25) Triolo, A.; Russina, O.; Fazio, B.; Triolo, R.; Di Cola, E. *Chem. Phys. Lett.* **2008**, 457, 362–365.

JP9022234